Highlights of Spanish Astrophysics VI, Proceedings of the IX Scientific Meeting of the Spanish Astronomical Society held on September 13 - 17, 2010, in Madrid, Spain. M. R. Zapatero Osorio et al. (eds.)

Magneto-acoustic wave energy in sunspots: observations and numerical simulations

Tobías Felipe[1,2], Elena Khomenko[1,2,3], Manuel Collados[1,2], and Christian Beck[1,2]

[1] Instituto de Astrofísica de Canarias, 38205, C/ Vía Láctea, s/n, La Laguna, Tenerife, Spain
[2] Departamento de Astrofísica, Universidad de La Laguna, 38205, La Laguna, Tenerife, Spain
[3] Main Astronomical Observatory, NAS, 03680, Kyiv, Ukraine

Abstract

We have reproduced some sunspot wave signatures obtained from spectropolarimetric observations through 3D MHD numerical simulations. The results of the simulations are compared with the oscillations observed simultaneously at different heights from the Si I λ 10827 Å line, He I λ 10830 Å line, the Ca II H core and the Fe I blends at the wings of the Ca II H line. The simulations show a remarkable agreement with the observations, and we have used them to quantify the energy contribution of the magneto-acoustic waves to the chromospheric heating in sunspots. Our findings indicate that the energy supplied by these waves is 5-10 times lower than the amount needed to balance the chromospheric radiative losses.

1 Introduction

Wave propagation is one of the most promising candidates to explain chromospheric heating. Several authors have studied the contribution of acoustic wave energy, finding different results. [9] evaluated the energy contribution of high frequency acoustic waves in quiet Sun regions from TRACE observations, and obtained an energy flux 10 times lower than the required amount. However, some works have argued that these authors have neglected a factor of 10 in the short-period energy flux due to the limited spatial resolution of TRACE [6, 10]. Recently, [4] obtained an acoustic flux at a height of 250 km above the photosphere only around 2 times lower than the chromospheric radiative losses.

In this work we aim to evaluate the energy supplied by magneto-acoustic waves to the chromosphere in sunspots regions. Our approach consist in using 3D numerical simulations to reproduce the oscillatory pattern from the photosphere to the chromosphere, detected from temporal series of spectropolarimetric data, and quantify the energy flux of these waves.

2 Observational and numerical procedures

The observational data consists of a temporal series of co-spatial and simultaneous data obtained on August 28$^{\text{th}}$ 2007 with two different instruments, the POlarimetric LIttrow Spectrograph (POLIS [3]) and the Tenerife Infrared Polarimeter II (TIP-II [5]), attached to the German Vacuum Tower telescope at the Observatorio del Teide at Tenerife. TIP-II provides Stokes spectra of the 10830 Å region, including the Si I λ 10827 Å and He I λ 10830 Å spectral lines, with a spatial sampling of $0\farcs18$ per pixel. The blue channel of POLIS obtains intensity spectra of the Ca II H λ 3968 Å line and some photospheric Fe I line blends in its wings, with a spatial sampling of $0\farcs29$ per pixel. The slit was placed over the center of a sunspot located near the center of the solar disk. A thorough analysis of this dataset was presented in [8].

We have performed 3D numerical simulations to reproduce the observed wave pattern from the photosphere to the chromosphere. The numerical method is described in detail in [7]. The code solves the nonlinear MHD equations for perturbations. An MHD model which resembles the properties of the observed sunspot is perturbed with a driver force in the momentum equation. We have introduced a driver force that reproduces the velocity measured with the Si I line, since it is the line formed at the largest depth over the set of lines that we have observed. The radiative energy losses are implemented following Newton's cooling law, with the radiative relaxation time taken from [12].

3 Analysis of the simulations

3.1 Configuration

In order to compare the numerical simulation with the observational data, we have assigned a fixed z to the formation height of each spectral line, and we have assumed that the vertical velocity at that location corresponds to the velocity measured from the Doppler shift of the line. We have introduced the driver at the formation height of the Si I line according to [2]. The geometrical distance to the rest of the observed spectral lines was retrieved from [8].

The computational domain covers 14.8×8.4 Mm in the horizontal directions, with a spatial step of $\Delta x = \Delta y = 100$ km. In the vertical direction it spans from $z = -0.6$ Mm to $z = 1$ Mm, with a spatial step of $\Delta z = 25$ km.

3.2 Comparison between observations and simulations

The vertical force introduced at the height of the Si I line formation mainly generates slow acoustic waves in the low-β region. The oscillatory pattern introduced in the simulation resembles remarkably well the LOS velocity measured with the Si I line, as shown in Fig. 1. Most of its power is concentrated in the 5 minute band, with frequencies between 3 and 4 mHz, and they form standing waves due to the higher cutoff frequency of the atmosphere. The driver also generates high frequencies waves, which propagate upward to the chromosphere. In their travel through the sunspot atmosphere, they reach the formation height of several observed spectral lines. The highest spectral line observed is the He I line. The comparison

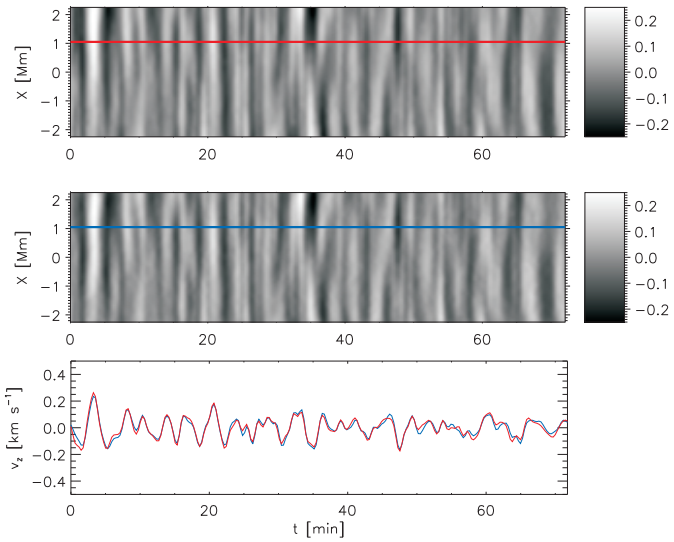

Figure 1: Velocity maps derived from the Si I line (vertical axis: slit direction; horizontal axis: time). *Top*: Observational, measured from the Doppler shift of the Si I line. *Middle*: numerical, vertical velocity at the formation height of the Si I line. *Bottom*: comparison of the observational (red line) and numerical (blue line) velocity at $x = 1.1$ Mm.

between the Doppler velocity of this line and the vertical velocity of the simulation at the corresponding height is given in Fig. 2. The He I core is formed at the chromosphere, so these waves have propagated upwards about 850 km from the formation height of the Si I line in order to reach this layer [8]. During this travel, the period of the waves is reduced to around 3 minutes and their amplitude increases, reaching peak-to-peak values of almost 8 km s^{-1}. Bottom panel of Fig. 2 shows that the oscillations develop into shocks. The simulated velocity map reproduces reasonably well the observed oscillatory pattern. Only those waves with frequecy above the cutoff can reach the chromosphere. The increase of the amplitude of these waves with height is higher than the one corresponding to the evanescent low frequency waves, and the power spectra at the chromosphere is dominated by a peak at 6 mHz.

Figure 3 shows the phase difference and amplification spectra between the photospheric Si I line and the chromospheric He I line, for both observational and simulated velocities. From 1 to 7 mHz, the simulated phase difference precisely matches the observed one, with a null phase difference for frequencies below 4 mHz and an almost linear increase between 4 and 7 mHz. At higher frequencies the coherence of the observed phase difference is lower, but the simulated one keeps its linear increase. Regarding the amplification spectra, for frequencies above 1.5 mHz the simulated spectra reproduces properly the observed one.

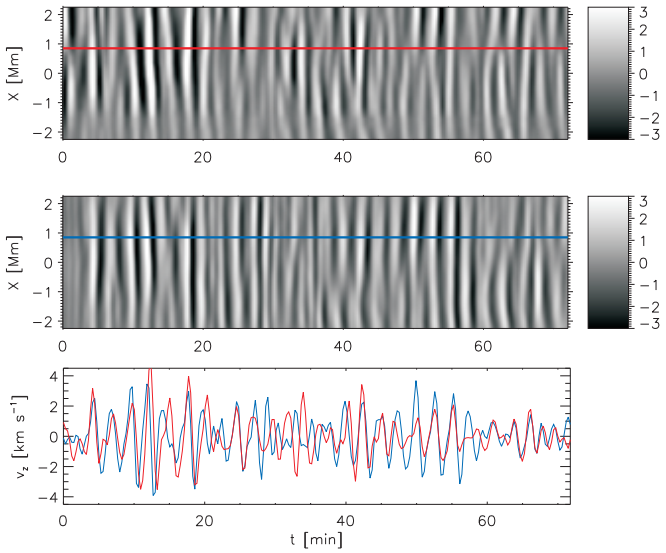

Figure 2: Velocity maps of the He I line (vertical axis: slit direction; horizontal axis: time). *Top*: Observational, measured from the Doppler shift of the He I line. *Middle*: numerical, vertical velocity at the formation height of the He I line. *Bottom*: comparison of the observational (red line) and numerical (blue line) velocity at $x = 0.9$ Mm.

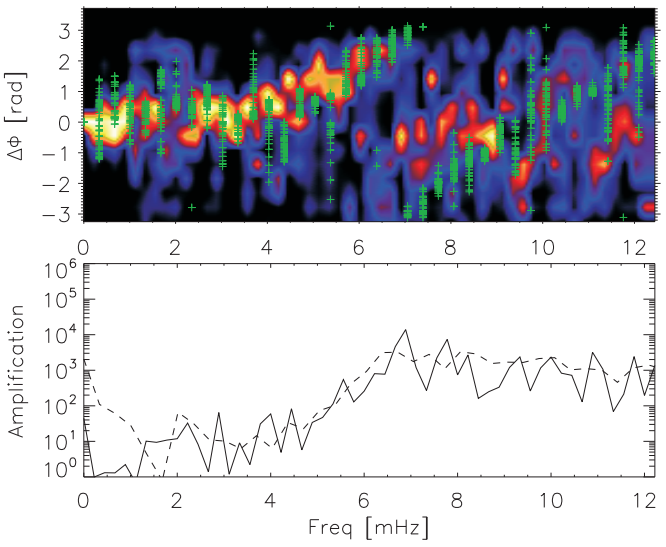

Figure 3: *Top*: Phase difference spectra between Si I and He I velocities in the umbra. The color code shows the relative occurrence of a given phase shift. The green crosses are the results of the simulation for all the spatial points. *Bottom*: Amplification spectra for the observation (black solid line) and the simulations (black dashed line).

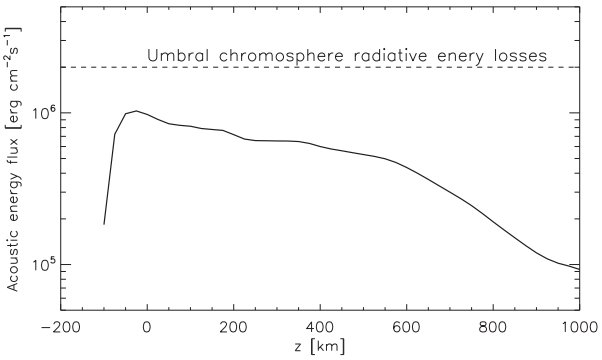

Figure 4: Spatially and temporally average acoustic energy flux inside the umbra in the simulation, calculated as $F_{\rm ac} =< p_1 \mathbf{v}_1 >$. The zero height corresponds to the quiet Sun surface.

3.3 Energy balance

The slow acoustic mode generated directly by the driver propagates upwards along the field lines. The cutoff frequency reaches a maximum value of $\nu_{\rm c} = 6$ mHz. It means that the oscillations in the 5 minute band introduced by the driver cannot propagate upwards, and they form evanescent waves which do not supply energy to the higher layers. Only those waves with frequency above the cutoff can propagate to the chromosphere.

During the travel of high frequency waves to high layers their amplitude increases due to the drop of the density and they develop into shocks with peak-to-peak amplitudes around 8 km s^{-1} at the formation height of the Ca II H core and the He I line. According to [1], the radiative energy losses in the umbral chromosphere amount to 2.6×10^6 erg cm^{-2} s^{-1}, while [11] estimate a similar value of 1–2 $\times 10^6$ erg cm^{-2} s^{-1}. These losses should be balanced by some energy source. Figure 4 illustrates the variation of the acoustic flux with height. It was averaged in time for all points inside the umbra. It grows up to 10^6 erg cm^{-2} s^{-1} just above the layer where the driver is introduced and decreases with height due to dissipation and radiative energy losses. At the chromospheric formation height of the He I line it is around 3×10^5 erg cm^{-2} s^{-1}, between 3 and 10 times lower than required to balance the chromospheric losses.

4 Discussion and conclusions

We have presented numerical simulations which closely reproduce the real wave propagation detected in the umbra of a sunspot from the photosphere to the chromosphere, and we have used this simulation to quantify the acoustic energy flux supplied to the chromosphere.

At the photospheric formation height of the Si I line most of the wave power is concentrated in the 5 minute band, with frequencies between 3 and 4 mHz, which corresponds to standing waves due to the higher cutoff frequency of the atmosphere. High-frequency waves (above 4 mHz) propagate upward to the chromosphere, and in their travel through

the sunspot atmosphere they reach the formation height of several observed spectral lines. Simulations reproduce reasonably well the velocity maps and power spectra at the formation heights of chromospheric Ca II H and He I and the photospheric Fe I lines. Our simulations reproduce the phase and amplification spectra between several pairs of lines with a remarkable match. For those spectra between a photospheric and a chromospheric signal, the phase difference shows stationary waves with $\Delta\phi = 0$ below 4 mHz. At higher frequencies the waves progressively propagate with $\Delta\phi$ increasing with the frequency.

The analysis of the energy flux carried by magnetoacoustic waves to high layers reveals that it is not enough to heat the chromosphere. The average energy supplied by slow acoustic waves is around 3 to 10 times lower than the amount required to balance the radiative losses, depending on the reference taken for the umbral chromospheric radiative losses. Previous works have found that the acoustic wave energy is too low, by a factor of at least ten, to balance the radiative losses in the non-magnetic solar chromosphere [9]. The fraction of the required energy supplied by acoustic waves in the magnetized atmosphere of a sunspot seems to be higher, but also insufficient. Figure 4 shows that at the formation height of the Si I line the average acoustic energy flux is around 10^6 erg cm^{-2} s^{-1}, so at this photospheric height the energy contained in form of acoustic waves is of the same order as magnitude of the amount required by the chromospheric radiative losses.

Acknowledgments

This research has been funded by the Spanish MICINN through projects AYA2010–18029 and AYA2010–18029. The simulations have been done on the La Palma supercomputer at Centro de Astrofísica de La Palma and on the MareNostrum supercomputer at the Barcelona Supercomputing Center.

References

[1] Avrett, E. H. 1981, in *The Physics of Sunspots*, ed. L. E. Cram & J. H. Thomas, 235

[2] Bard, S., & Carlsson, M. 2008, ApJ, 682, 1376

[3] Beck, C., Schmidt, W., Kentischer, T., & Elmore, D. 2005, A&A, 437, 1159

[4] Bello González, N., Franz, M., & Martínez Pillet, V. 2010, ApJ, 723, L134

[5] Collados, M., Lagg, A., & Díaz García, J. J., 2007, in *The Physics of Chromospheric Plasmas*, ASP Conf. Ser., Vol. 368, ed. P. Heinzel, I. Dorotovič, & R. J. Rutten, 611

[6] Cuntz, M., Rammacher, W., & Musielak, Z. E. 2007, ApJ, 657, L57

[7] Felipe, T., Khomenko, E., & Collados, M. 2010a, ApJ, 719, 357

[8] Felipe, T., Khomenko, E., Collados, M., & Beck, C. 2010b, ApJ, 722, 131

[9] Fossum, A., & Carlsson, M. 2005, Nature, 435, 919

[10] Kalkofen, W. 2007, ApJ, 671, 2154

[11] Kneer, F., Mattig, W., & v. Uexkuell, M. 1981, A&A, 102, 147

[12] Spiegel, E. A. 1957, ApJ, 126, 202